Nonlin. Processes Geophys., 13, 247–253, 2006
www.nonlin-processes-geophys.net/13/247/2006/

Nonlinear Processes in Geophysics

A theoretical model of a wake of a body towed in a stratified fluid at large Reynolds and Froude numbers

Y. I. Troitskaya, O. A. Druzhinin, D. A. Sergeev, V. V. Papko, and G. N. Balandina

Institute of Applied Physics, Nizhny Novgorod, Russian Federation, Russia

Received: 30 September 2005 – Revised: 3 May 2006 – Accepted: 3 May 2006 – Published: 30 June 2006

Part of Special Issue "Turbulent transport in geosciences"

Abstract. The objective of the present paper is to develop a theoretical model describing the evolution of a turbulent wake behind a towed sphere in a stably stratified fluid at large Froude and Reynolds numbers. The wake flow is considered as a quasi two-dimensional (2-D) turbulent jet flow whose dynamics is governed by the momentum transfer from the mean flow to a quasi-2-D sinuous mode growing due to hydrodynamic instability. The model employs a quasi-linear approximation to describe this momentum transfer. The model scaling coefficients are defined with the use of available experimental data, and the performance of the model is verified by comparison with the results of a direct numerical simulation of a 2-D turbulent jet flow. The model prediction for the temporal development of the wake axis mean velocity is found to be in good agreement with the experimental data obtained by Spedding (1997).

1 Introduction

Laboratory studies of turbulent stratified wakes have been carried out since late 1960s (Lin and Pao, 1979; Boyer and Srdic-Mitrovic, 2001; Sysoeva and Chashechkin, 1991; Chomaz et al., 1993; Lin et al., 1992; Bonneton et al., 1993; Lin et al., 19993; Hopfinger et al., 1991; Robey, 1997; Spedding et al., 1996; Spedding, 1997; Bonnier and Eiff, 2002; Riley and Lelong, 2000; Lilly, 1983; Embid and Majda, 1998; Fincham and Spedding, 1997; Spedding, 2001, 2002; Gourlay et al., 2001). The results of these studies show that there are three distinct regimes of the wake evolution which are defined with respect to the product Nt, where N is the characteristic value of the buoyancy frequency at the level of towing and t is the time elapsed from the moment of the body pass at a given point. In the near wake, at times $Nt\sim 1$, the fluid motion is three dimensional and there occurs a collapse of the vertical velocity pulsations due to the action of the buoyancy forces. The regime of the far wake takes place at large enough times (for $Nt>>1$), when the fluid motion becomes quasi two-dimensional. In the latter regime, the fluid motion occurs mostly in the horizontal layers so that the horizontal velocity component is larger then the vertical component. In this case, the viscous dissipation due to the large vertical velocity gradients becomes considerable. At intermediate times, there occurs also an intermediate stage of the wake evolution, where the wake flow is qualitatively changed due to transition from 3-D to the quasi-2-D motion.

Correspondence to: Y. I. Troitskaya
(yuliya@hydro.appl.sci-nnov.ru)

Experimental results (Spedding et al., 1996; Spedding, 1997; Bonnier and Eiff, 2002) show that at large enough Froude and Reynolds numbers of the towed sphere, $Fr={}^{2U_t}\!/_{ND}$ and $Re={}^{U_t D}\!/_{\nu}$ (where D is the sphere diameter, U_t the towing speed, and ν the fluid molecular viscosity) the temporal development of the mean velocity maximum at the wake axis $U_0(t)$ depends on time as: $U_0(t)\sim t^{-2/3}$ in the three-dimensional near wake region; as $U_0(t)\sim t^{-0.25}$ (Spedding, 1997) or $U_0(t)\sim t^{-0.38}$ (Bonnier and Eiff, 2002) in the transitional region; and as $U_0(t)\sim t^{-0.76}$ (Spedding, 1997) or $U_0(t)\sim t^{-0.9}$ (Bonnier and Eiff, 2002) in the far wake region. The experimental results also show that the fluid flow in the far wake is confined to a horizontal plane and consists of flat vortices of different polarity arranged in a "chess" order in the vicinity of the wake axis.

Although there has been a considerable progress in experimental and numerical studies of the far stratified wakes, a theoretical model is still needed to explain the properties of the wake evolution. An important role of the hydrodynamic instability in the wake dynamics was pointed out by Spedding (2002) who studied the streamlines patterns of the wake flow. His experimental results show that the wake evolution is accompanied by the growth of a quasi-2-D instability mode of the flow. This growth leads to the development of a sinous 2-D structure of flow streamlines in the plane of towing at

Published by Copernicus GmbH on behalf of the European Geosciences Union and the American Geophysical Union.

sufficiently large times. The objective of the present paper is to employ these experimental observation by Spedding and develop a theoretical model, describing the the wake evolution at the intermediate stage, i.e. for $Nt<50$. We assume that at this stage the wake dynamics is governed by the development of a quasi-2-D hydrodynamic instability mode. We neglect the effect of internal waves on the wake evolution (which is known to be insignificant at times $Nt\gg 1$) and consider the wake as a jet-like flow subject to quasi-2-D disturbances. Thus the reduction of the wake mean axis velocity is caused by the momentum transfer from the mean flow to the disturbances. The model also neglects the viscous dissipation associated with the vertical shear. Thus, the model is not applicable in the far wake region [for $Nt=O(100)$], where this dissipation is known to be significant (Riley and Lelong, 2000).

The paper is organized as follows. In Sect. 2 the model equations are presented. In Sect. 3 we verify the performance of the model by comparison of the model predictions with results of a direct numerical simulation of a 2-D turbulent jet flow. Finally, we compare the model predictions with the available experimental results in Sect. 4.

2 A theoretical model of the evolution of a quasi-two dimensional wake in a stratified fluid

Let us consider the far wake evolution taking into account only quasi two-dimensional (2-D) vorticity mode and neglecting its interaction with the internal-waves mode. As it was shown in Lilly (1983); Embid and Majda (1998), at large Richardson numbers the horizontal velocity field in the vortex mode is governed by a set of quasi-2-D hydrodynamics equations. When averaged over an ensemble of turbulent wake flow realizations, these equations can be written in terms of the mean stream function ψ and vorticity Ω as follows:

$$\frac{\partial\Omega}{\partial t}+\frac{\partial\psi}{\partial y}\frac{\partial\Omega}{\partial x}-\frac{\partial\psi}{\partial x}\frac{\partial\Omega}{\partial y}=\left(\frac{\partial^2}{\partial x^2}+\frac{\partial^2}{\partial y^2}\right)K_T\Omega+ + 2\left(2\frac{\partial^2 K_T}{\partial x\,\partial y}\frac{\partial^2\psi}{\partial x\,\partial y}-\frac{\partial^2 K_T}{\partial x^2}\frac{\partial^2\psi}{\partial y^2}-\frac{\partial^2 K_T}{\partial y^2}\frac{\partial^2\psi}{\partial x^2}\right) \tag{1a}$$

$$\frac{\partial^2\psi}{\partial x^2}+\frac{\partial^2\psi}{\partial y^2}=-\Omega, \tag{1b}$$

where K_T is the eddy viscosity coefficient. Note that in Eq. (1a) we neglect the vertical turbulent momentum transfer since the vertical velocity fluctuation component is known to be negligible compared to the horizontal component (Spedding, 2001, 2002).

Since the velocity of the sphere is typically much larger then the defect velocity in the wake, the statistical properties of the wake flow can be considered as homogeneous with respect to the longitudinal (x) coordinate. Thus we consider the wake mean flow velocity to be a function of y, z and t. The eddy viscosity coefficient also can be supposed to be independent of x.

We consider the wake flow as a quasi-2-D turbulent jet flow which is subject to a quasi-2-D disturbance. The growth of the disturbance occurs via hydrodynamic instability and is accompanied by a momentum exchange with the mean flow. We employ a quasi-linear approximation (Galeev and Sagdeev, 1973) and seek the solution to the set of Eqs. (1a, b) as a sum of a mean flow which does not depend on x coordinate, and the disturbance which is presented as a sum of harmonics in the form:

$$\psi(x,y,t)=\psi_0(y,\ t) + Re\sum_k a(k,\ t)\psi_1(y,\ t,\ k)\ \exp(ikx+i\varphi_k), \tag{2a}$$

$$\Omega\ (x,y,t)=\Omega_0(y,\ t) + Re\sum_k a(k,\ t)\Omega_1(y,\ t,\ k)\ \exp(ikx+i\varphi_k) \tag{2b}$$

where k is the wave number of the k-th harmonics, and the harmonics phases φ_k are random numbers.

The system of equations derived within the framework of the quasi-linear approximation includes firstly the equation for the mean flow velocity $U(y,t)=\frac{\partial\psi_0}{\partial y}$. This equation is obtained by averaging Eq. (1a) over x in the form:

$$\frac{\partial U}{\partial t}-\frac{\partial}{\partial y}\frac{1}{2}\sum_k k\,|a(k,t)|^2\,Im\ \left(\psi_1(y,t,k)\frac{\partial\psi_1}{\partial y}\right) =\frac{\partial}{\partial y}\left(K_T\frac{\partial U}{\partial y}\right). \tag{3}$$

We assume further that the characteristic time scale of the disturbance is much less than the characteristic time scale of the mean flow, so that the dependence of the complex amplitudes $\psi_1(y,t,k)$ on time can be described in the WKB-approximation (Galeev and Sagdeev, 1973). Then $\psi_1\,(y,t,k)=\Phi_0\,(y,t,k)\,e^{-i\int_0^t\omega(t,k)dt}$ and in the zero-th order of the WKB-approximation we obtain an eigenvalue boundary problem for amplitude Φ_0 and frequency ω in the form:

$$\Phi_0|_{y\to\pm\infty}=0. \tag{4}$$

The 1-st order of the WKB-approximation yields also the following equation for the amplitude a:

$$\int_{-\infty}^{\infty}\psi\frac{\partial}{\partial t}\left(a\left(\frac{\partial^2\Phi_0}{\partial y^2}-k^2\Phi_0\right)\right)dy=0, \tag{5}$$

where function $\psi\ (k,y)$ is the solution to the equation conjugated to Eq. (4). A more detailed derivation of the Eqs. (3–6) is provided in Balandina et al. (2004).

The model Eqs. (3–6) are solved numerically. Equation (3) for the mean velocity is solved by the Gauss method. The boundary problem Eqs. (4) and (5) is also solved at each time step for each spectral harmonics, whereby the eigenvalues $c\,(k)$ and eigenfunctions $\Phi_0(k, y)$ are evaluated. Coeffcient $a\,(k, t)$ is obtained from Eq. (6) in the form:

$$a\,(k,t) = a_0\,(k)\exp\left\{\int_0^t \frac{\int_{-\infty}^{\infty} \psi \frac{\partial \chi_0}{\partial t} dy}{\int_{-\infty}^{\infty} \psi \chi_0 dy} dt\right\},$$

where $\chi_0 = \frac{\partial^2 \Phi_0}{\partial y^2} - k^2 \Phi_0$.

Thus functions $a\,(k, t)$, Φ_0 and eigenvalue ω are computed and the equation for the mean velocity is solved numerically at each time step. At the initial time moment we prescribe a Gaussian profile of the mean velocity in the form:

$$U(y,0) = U_{00}\exp\left(-y^2\big/\delta_0^2\right) \quad (6)$$

and the disturbance spectrum in the form:

$$a_0\,(k) = \varepsilon_{00}\delta_0^2 k e^{-k\delta_0/K_0} \quad (7)$$

where U_{00} is the initial mean velocity, ε_{00} the spectral amplitude,δ_0 the initial wake width, and wave number K_0 defines the initial location of the spectrum maximum. Parameters ε_{00} and K_0 as well as the eddy viscosity coefficient $K_T$are defined further to match the numerical and experimental data.

3 Numerical simulation of a temporally-developing 2-D turbulent jet flow

In order to verify the theoretical model discussed above, we perform direct numerical simulation (DNS) of a 2-D turbulent jet flow. We consider a flow with reference profile of the longitudinal (x) velocity component in the dimensionless form:

$$U_{\text{ref}} = -\exp(-4y^2), \quad (8)$$

where y is the lateral coordinate. The flow is assumed to be periodic in the x-direction. The initial fluid velocity is prescribed as a sum of the reference velocity (Eq. 9) and a fluctuation velocity component. The latter is given by the sum of independent Fourier harmonics with random phases and a power spectrum $[E(k) \sim E_0 k^4 \exp(-2k)]$ where k is the wave number modulus ($k^2 = k_x^2 + k_y^2$). Thus, spectrum $E(k)$ has a maximum at k=2 which corresponds to the most unstable mode of the flow. The velocity fluctuation distribution is made proportional to the reference profile (Eq. 9), and its amplitude is prescribed to be of the order of 20% of the reference velocity maximum which is in accordance with the experimentally observed value of the velocity fluctuation in the wake flow.

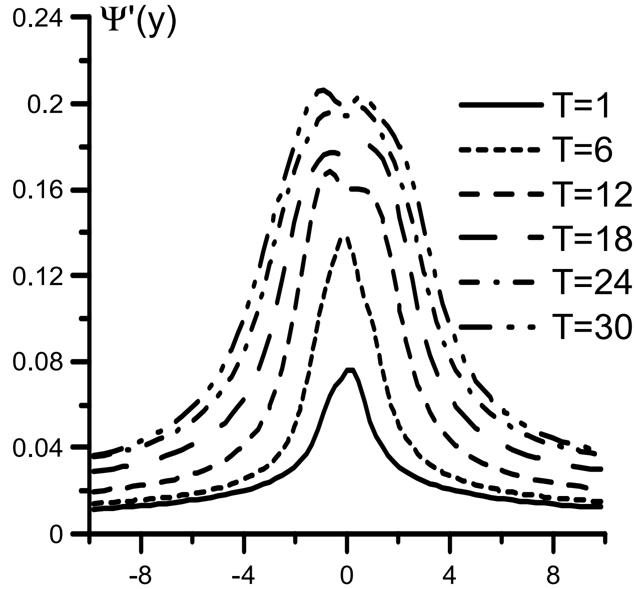

Fig. 1. Profiles of the rms deviation of the stream function in DNS.

The 2-D Navier-Stokes equations and the incompressibility condition for the fluid velocity are discretized and solved in a rectangular domain with the use of a pseudo-spectral method on a staggered grid consisting of 1200×320 nodes in the x- and y-directions, respectively. The grid is uniform in the x-direction and non-uniform in the y-direction, so that the grid is isotropic in the vicinity of the jet axis and the grid spacing increases towards the domain boundaries in the y-direction. The integration is advanced in time with the use of the Adams-Bashforth method with time step Δt=0.0075, and the grid spacing equals Δx=0.075. The shear-free (Neumann) boundary condition is prescribed over the lateral coordinate. The flow Reynolds number Re is prescribed to be equal to Re=400, so that the effects of fluid molecular viscosity remain sufficiently small during the simulation time. More details of the numerical algorithm are provided in Druzhinin (2003).

The DNS was performed for 10 different initial distributions of the fluid velocity fluctuation field. Figure 1 shows the profiles of the rms deviation of the stream function from its mean value evaluated at consequent time moments for each y as:

$$\psi'(y,t) = \left\langle (\psi\,(x,y,t) - \langle\psi\,(y,t)\rangle)^2 \right\rangle^{1/2}. \quad (9)$$

Here the averaging is first performed over 10 different realizations of the flow field and then the x-averaged value is computed, so that:

$$\langle\cdots\rangle = \frac{1}{10L_x}\sum_{i=1}^{10}\int \cdots dx. \quad (10)$$

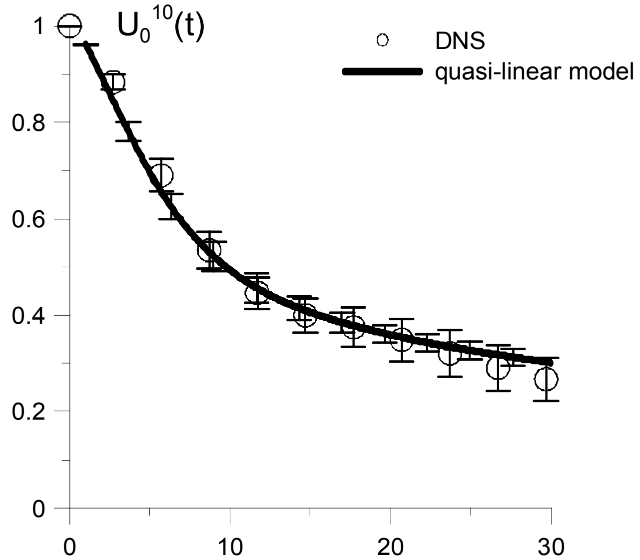

Fig. 2. Temporal development of the mean velocity at the axis of the 2-D turbulent jet. Symbols represent the DNS results averaged over 10 different runs. Solid curve corresponds to the model prediction.

In the case of a sinuous mode, the stream function disturbance is an even function of y whose maximum is at y=0, and for the "varicose" mode it is an odd function with zero at y=0. Figure 1 shows that initially at T=0 function ψ' has its maximum at y=0, and later (for T=18) a local minimum of ψ' appears at y=0. Therefore, the figure shows that the sinuous mode is mainly exited and prevails over the varicose mode.

In order to compare the DNS results and the model prediction we prescribed the initial spectra $\varepsilon_0^{(i)}(K)$ in accordance with the initial spectra of the flow disturbance in each DNS run and evaluated the wake axis velocity and spectra of the disturbance at different time moments. Figure 2 shows the temporal development of the wake axis velocity averaged over the solutions provided by the model for each initial spectrum $\varepsilon_0^{(i)}(K)$ and eddy viscosity coefficient K_T=200. The figure shows that the model prediction is in good agreement with the DNS results.

Figure 3 shows the spectra of the stream function obtained in DNS at different time moments and averaged over 10 runs and the corresponding model solution. The figure shows that there is a difference between the model prediction and the DNS results in that the model spectra grow more rapidly in the regions of small and large wave numbers. The latter difference can be explained by the nonlinear harmonics interaction which is not taken into account by the model. However, the figure shows that the model solution correctly describes the main features of the temporal evolution of the energy peak wave number and the amplitude of the peak.

We should point out that the good agreement of the quasi-linear model and DNS results can be explained also by the properties of the interaction of the harmonics with random phases. Indeed, in this case, the harmonics interact on a slower timescale, which results in a relatively small nonlinear effects, even if the flow Reynolds number is comparatively large.

4 Comparison of the model prediction for the wake axis velocity with the experimental data

As follows from the discussion in Sect. 2, the theoretical model provides a solution for the wake axis velocity in the form $U(t)$=$U_{00}\theta\left(\frac{U_{00}t}{\delta_0}\right)$. On the other hand, the results of the laboratory studies of the wake of a sphere towed in a stratified fluid at different Froude (Fr) numbers (Spedding, 1997) show that the temporal development of the wake axis velocity can be represented in the form:

$$U_0(t) = \gamma U_t Fr^{-2/3}\Phi(Nt) \tag{11}$$

where U_t is the towing speed, N the buoyancy frequency, and γ is a constant factor. Since dimensionless time $T\equiv\frac{U_{00}t}{\delta_0}$ is proportional to Nt , so that T=αNt, where α is a constant factor, Eq. (11) can be rewritten in the following equivalent form:

$$\frac{U_0(t)}{U_t Fr^{-2/3}} = \gamma\theta(\alpha Nt). \tag{12}$$

Equation (12) shows that in order to compare the model prediction for the wake axis velocity with the experimental results (Spedding, 1997) we need to define constant factors α and γ. Therefore, we performed a laboratory experiment where we studied the flow field in the wake of a sphere and ellipsoid towed in a salt-stratified fluid at large Froude and Reynolds numbers which enabled us to determine factors α and γ (Balandina et al., 2004). In these experiments, the body diameter was varied in the range from 0.8 cm to 1.3 cm, and towing speed was in the interval from 34 cm/s to 98 cm/s. Thus the Froude number varied from 17 to 88, and the Reynolds number varied from 3760 to 8000, respectively. The velocity field was measured in the horizontal plane at the level of towing with the use of the PIV method. More details of the description of the experimental setup are provided in Balandina et al. (2004).

The mean velocity profile obtained in the experiment at a given time moment t was evaluated by spatial averaging over the longitudinal coordinate x and was approximated by a Gaussian curve. Thus, the temporal development of the wake axis velocity U_0 was obtained both as a function of Nt and a function of T=$t\frac{U_{00}}{\delta_0}$.

Figure 4a shows the temporal development of the wake mean axis velocity obtained in the experiment for different Froude numbers (in symbols) and the model solution for $U_0(T)$ (solid curve) normalized by the initial velocity. The model parameter ε_{00}=0.106 in accordance with the velocity fluctuations spectra measured in the experiment. The

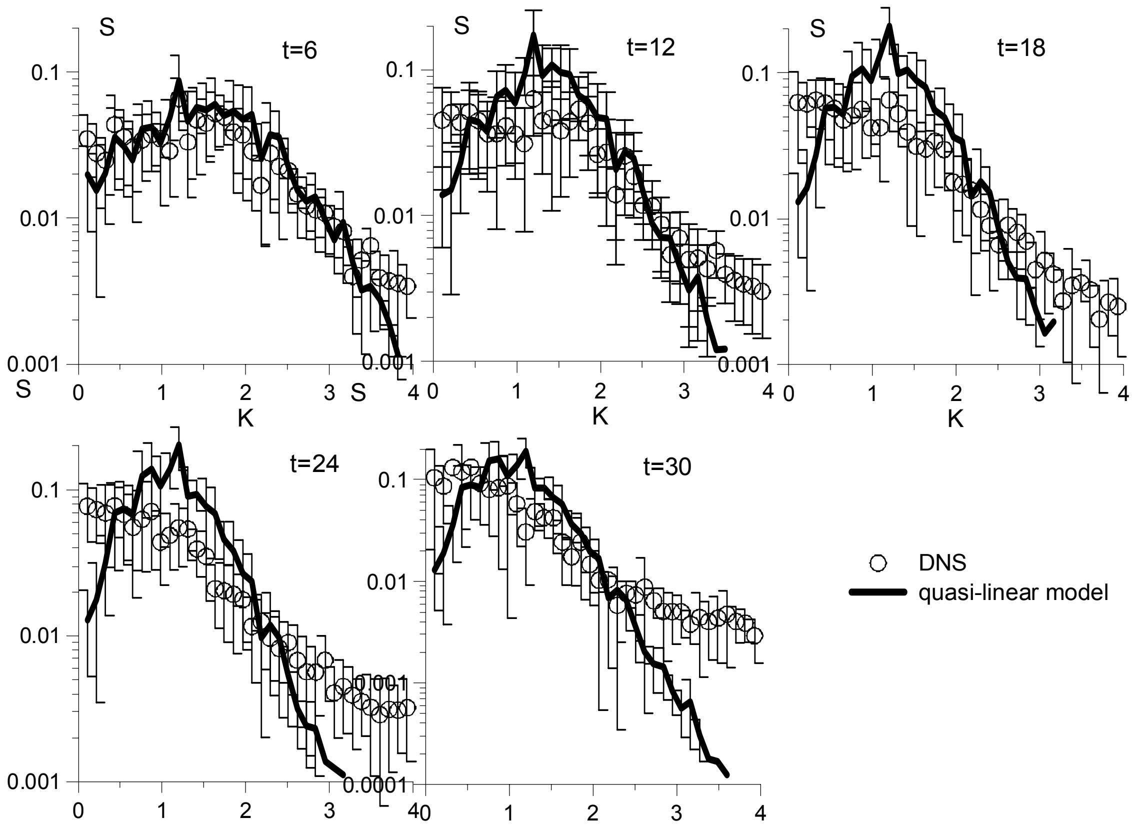

Fig. 3. The spectra of the stream function disturbance at different time moments in DNS (symbols) and the model solution (solid curve).

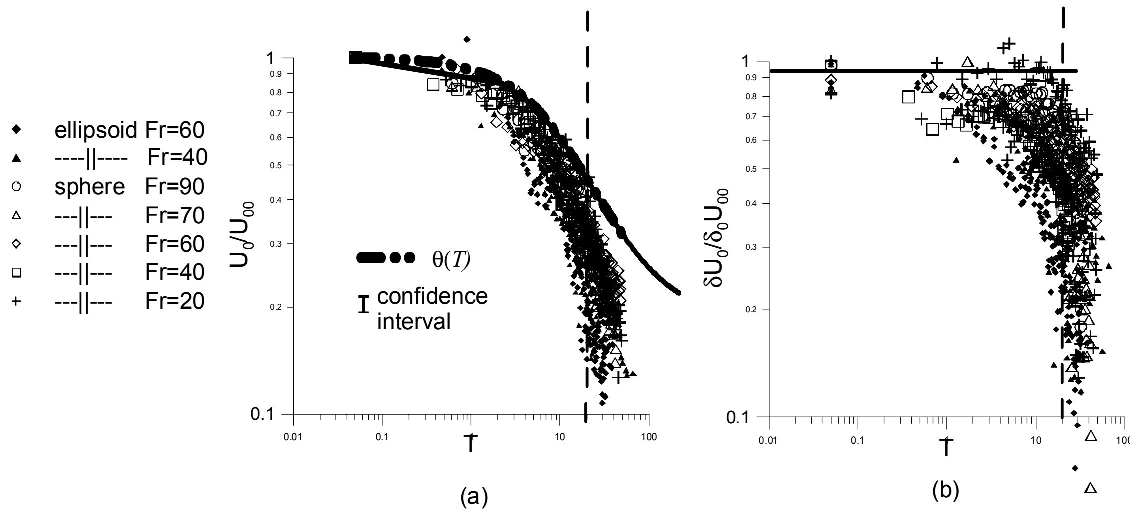

Fig. 4. **(a)** experimental data (symbols) and model solution (soluid curve) for the wake axis velocity; the approximation of the velocity by function $\theta(T)$ (Eq. 13) is shown in dash-dotted curve; **(b)** temporal development of the product $U_0(T)\delta(T)$ in the experiment.

figure shows a good agreement between the model prediction and our experimental results at times $T<20$. However, the model over predicts the mean velocity at later times. This can be explained by the assumption of the model to neglect vertical diffusion of the vorticity. In consequence, the wake momentum integral is conserved and the product $U_0(T)\delta(T)$=const. The temporal development of this product is shown in Fig. 4b. The figure shows that for

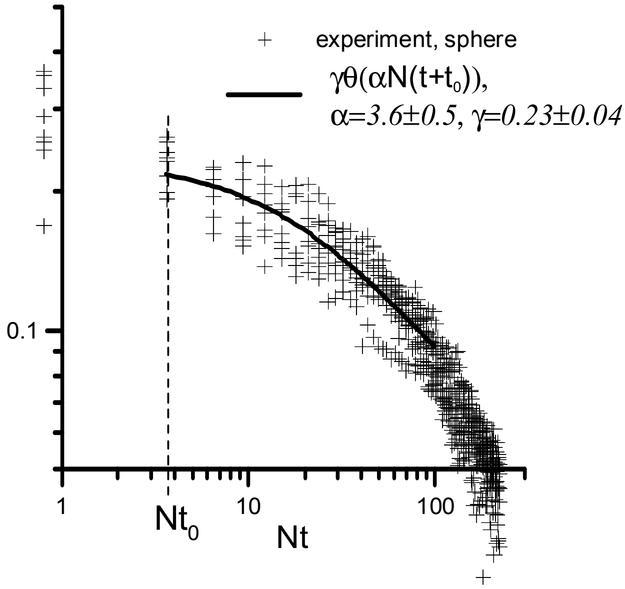

Fig. 5. Approximation of the experimental points by the function $\theta(T)$ (Eq. 13).

$T>20$the product $U_0(t)\delta(t)$ decreases substantially. Therefore, at this stage the vertical diffusion effects become essential and needs to be taken into account.

For convenience we employ the following approximation function for the normalized wake axis velocity $U_0(T)/U_{00}$:

$$\theta(T)=\frac{1+0.018T}{1+0.0989T} \tag{13}$$

This function is shown in Fig. 4a in dashed-dotted curve. This function is employed further to approximate the experimental data and determine coefficients $\gamma,\ \alpha$.

In order to determine coefficients $\gamma,\ \alpha$ in Eq. (12) we represent the experimental data for the velocity obtained for different *Re* and *Fr* numbers as a function of dimensionless time *Nt* in Fig. 5. The figure shows that experimental data points are collapsed by scaling Eq. (12) for α=3.6±0.5 and γ=0.23±0.04.

Figure 6 compares the prediction of the model (in solid curve) with experimental results obtained by Spedding (1997) (symbols). The figure shows also the asymptotics $U_0(t)\sim t^{-0.25}$ and $U_0(t)\sim t^{-0.76}$ introduced by Spedding (1997) to describe the temporal development of the wake axis velocity in the transitional and far-wake regions. The figure shows that the model results agree well with both the experimental data and the asympotics.

5 Conclusion

We have developed a theoretical model describing the evolution of a turbulent wake behind a towed sphere in a stably stratified fluid at large Froude and Reynolds numbers. The model assumption is that the wake flow dynamics in the transitional region (i.e. for *Nt*<50) is similar to the dynamics of as a quasi two-dimensional (2-D) turbulent jet flow and is governed by the momentum transfer from the mean flow to a quasi-2-D sinuous mode growing due to hydrodynamic instability. The model employs a quasi-linear approximation to describe this momentum transfer. The model scaling coefficients are defined with the use of available experimental data, and the performance of the model is verified by comparison with the results of a direct numerical simulation of a 2-D turbulent jet flow. The model prediction for the temporal development of the wake axis mean velocity is found to be in good agreement with the experimental data obtained by Spedding (1997).

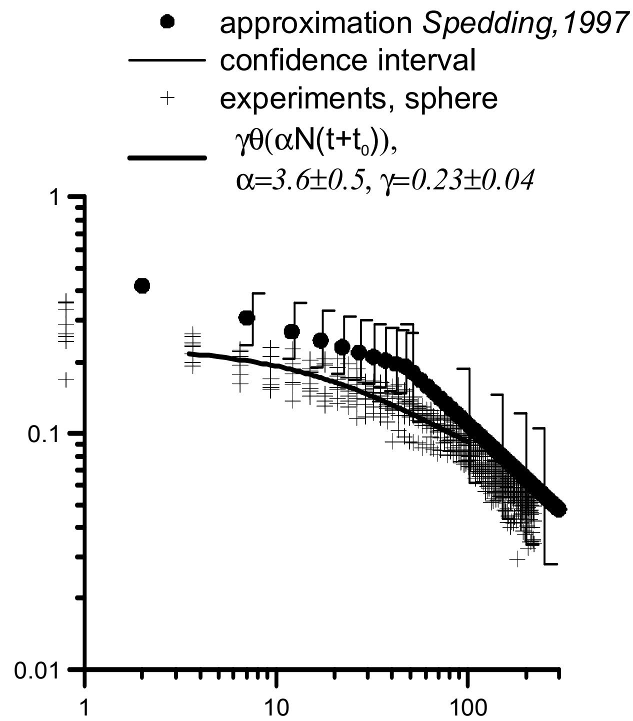

Fig. 6. The temporal development of the wake axis velocity according to the experimental data (Spedding, 1997) (crosses), asymptotics $U_0(t)\sim t^{-0.25}$ and $U_0(t)\sim t^{-0.76}$ (bullets) and the model prediction (solid curve). Vertical bars show the accuracy of the asymptotics introduced in Spedding (1997).

Acknowledgements. We are grateful to an anonymous referee for useful remarks. This work was carried out under the support of RFBR (project codes 04-05-64264 and 06-05-64890) and the Russian Science Support Foundation.

Edited by: J.-B. Flor
Reviewed by: two referees

References

Balandina, G. N., Papko, V. V., Sergeev, D. A., and Troitskaya, Y. I.: Evolution of the far turbulent wake behind a body towed in stratified fluid with large Reynolds and Froude numbers, Izv. Atmos. Oceanic Phys., 40(1), 99–113, 2004.

Bonneton, P., Chomaz, J. M., and Hopfinger, E. J.: Internal waves produced by the turbulent wake of a sphere moving horisontally in a stratified fluid, J. Fluid Mech., 254, 23–40, 1993.

Bonnier, M. and Eiff, O.: Experimental investigation of the collapse of a turbulent wake in a stably stratified fluid, Phys. Fluids., 14(N2), 791–801, 2002.

Boyer, D. L. and Srdic-Mitrovic, A.: Laboratory studies of continuously stratified flows past obstacles, Chapter 7, in: Environmental Stratified Flows, edited by: Grimshaw, R., Kluwer Acad. Publ., 191–222, 2001.

Chomaz, J. M., Bonneton, P., and Hopfinger, E. J.: The structure of the near wake of a sphere moving horisontally in a stratified fluid, J. Fluid Mech., 254, 1–21, 1993.

Druzhinin, O. A.: Collapse and self-similarity of a turbulent jet in a picnocline, Izv. Atmos. Oceanic Phys., 35(5), 629–641, 2003.

Embid, P. F. and Majda, A. J.: Low froude number limiting dynamics for stably stratified flows with small or finite Rossby numbers, Geophys. Astrophys. Fluid Dyn., 87, 1–50, 1998.

Fincham, A. M. and Spedding, G. R.: Low–cost, high–resolution DPIV for turbulent flows, Exps.Fluids., 23, 449–462, 1997.

Galeev, A. A. and Sagdeev, R. Z.: Nonlinear theory of plasma, Questions of theory of plasma. I.: Energoatomizdat, 7, 3–145, 1973.

Gourlay, M. J., Arendt, S. C., Fritts, D. C., and Werne, J.: Numerical modeling of initially turbulent wakes with net momentum, Phys. Fluids., 13(8), 2361–2372, 2001.

Hopfinger, E. J., Flor, J. B., Chomaz, J. M., and Bonneton, P.: Internal waves generated by a moving sphere and its wake in a stratified fluid, ExP. Fluids, 11, 255–261, 1991.

Lilly, D. K.: Stratified turbulence and the mesoscale variability of the atmosphere, J. Atmos.Sci., 40, 749–761, 1983.

Lin, J.–T. and Pao, Y.–H.: Wakes in stratified fluids, Ann. Rev. Fluid Mech., 11, 317–338, 1979.

Lin, Q., Lindberg, W. R., Boyer, D. L., and Fernando, H. J. S.: Stratified flow past a sphere, J. Fluid Mech., 240, 315–354, 1992.

Lin, Q., Boyer, D. L., and Fernando, H. J. S.: Internal waves generated by the turbulent wake of a sphere, ExP. Fluids, 15, 147–154, 1993.

Riley, J. J. and Lelong, M.-P.: Fluid motions in the presence of strong stable stratification, Annu. ReV. Fluid Mech., 32, 613–657, 2000.

Robey, H. F.: The generation of internal waves by a towed sphere and its wake in a thermocline, Phys. Fluids., 9(11), 3353–3367, 1997.

Spedding, G. R., Browand, F. K., and Fincham, A. M.: Turbulence, similarity scaling and vortex geometry in the wake of a towed sphere in a stably stratified fluid, J. Fluid Mech., 314, 53–103, 1996.

Spedding, G. R.: The evolution of initially-turbulent bluff-body wakes at high internal Froude numbe, J. Fluid Mech., 337, 283–301, 1997.

Spedding, G. R.: Anisotropy in turbulence profiles of stratified wakes, Phys. Fluids., 13(8), 2361–2372, 2001.

Spedding, G. R.: Vertical structure in stratified wakes with high initial Froude number, J. Fluid Mech., 454, 71–112, 2002.

Sysoeva, E. Y. and Chashechkin, Y. D.: Vortex systems in the stratified wake of a sphere, IzV. Akad. Nauk SSSR, Mekh. Zhidk. Gaza, 4, 82–90, 1991.